Renewable Energy 71 (2014) 679–689

Contents lists available at ScienceDirect

Renewable Energy

journal homepage: www.elsevier.com/locate/renene

Impacts of reforming energy subsidies on small scale generator business in Iran

M. Shahverdi [a, *], S.M. Moghaddas-Tafreshi [b], Michael S. Mazzola [a], A.K. Kaviani [c]

[a] Electrical and Computer Engineering Department, Mississippi State University, Mississippi State, MS 39762, USA
[b] Department of Electrical Engineering, K.N. Toosi University of Technology, Tehran, Iran
[c] Battery Management Department, Qualcomm, San Diego, CA, USA

ARTICLE INFO

Article history:
Received 5 January 2014
Accepted 22 June 2014
Available online 9 July 2014

Keywords:
Iran
Optimal strategy
Subsidies

ABSTRACT

Iran had been dedicating a substantial amount of its budget, known as subsidy, to keep the price of natural gas and electricity for customers considerably lower than real cost until 2011. Legislatures passed a law reforming energy subsidy in 2011, but this process is to take five years. Iran ceased to fully-subsidize from 2011, and gradually continues this process through 2015 when no subsidy will be paid. After 2015, the energy price will reach its prime cost. In addition, Tavanir organization, official organization of electrical energy management, published the "contract of guaranteed purchase price of energy for small scale generator". Based on the contract, the Ministry of Energy guaranties that electricity generated by a small scale generator is purchased at a price higher than market purchase price (http://www.tavanir.org.ir: letter no. 52504/350, October 22, 2008). These two issues, reforming subsidies and incentives for small scale generators' owners, would affect distributed generation areas in terms of operation and investment. This research studies effects of reforming energy subsidy on optimum daily operation of a Fuel Cell Power Plant (FCPP), as an example; however, the results are not only helpful for FCPP but also extendable to some extent to other small scale distributed generators.

1. Introduction

Two main reasons motivate authors to study optimal operations of small scale generators in Iran distributed system. First, before removing subsidies, end users have been supplied by conventional power plants since this is the cheapest way of producing electricity; however, reforming subsidies raises electricity purchase tariff and would open new opportunities for small scale generators, so they are able to compete with conventional power plants. Therefore, operational costs of small scale generators need to be evaluated in light of reforming the energy subsidy. Next, ministry of energy (MOE) guaranties that electricity produced by a small scale generator will be purchased at a price higher than regular market purchase price [1]. This guarantee encouraged the authors to study operational strategy of a small scale generator. There are other factors that encourage this study, one of which is privatization; according to article 44 of Iranian constitution, the government is urged to transfer ownership of power plants and some other properties from the public sector to the private sector. Therefore, MOE, after selling power plants, has to support the private sector by making policies because these small or large power plants are critically important from consumers' prospective. Furthermore, Tavanir organization reports that Iran annually needs approximately 10% more electrical energy which shows real need for purchasing electricity from new power plants such as small scale generators.

An economic model of FCPP operation is applied in this study in order to evaluate the situation of small scale generators when reforming energy subsidies. Although the exact impacts on other types of generation units cannot be evaluated by this study, the similar impacts can be seen. FCPP efficiently generates electricity with no pollution [2–4] as well as producing hydrogen, which also can be sold at the end of each day. The economic model of grid-parallel PEM fuel cells was previously studied [5–7]. This economic model has been improved. First, this model has been extended in Ref. [8,9] to study the effects of variable purchased/sold electricity tariffs. The model also was improved to recover thermal power from both reformer and PEM.

The Artificial neural networks (ANNS) [10], evolutionary programming (EP) and Hill climbing techniques (HC) [5,6] were examined to determine economic operation strategies of distributed

* Corresponding author. Tel.: +1 6626179761.
E-mail addresses: ms1626@msstate.edu, masood.shahverdi@gmail.com (M. Shahverdi).

http://dx.doi.org/10.1016/j.renene.2014.06.036
0960-1481/

Nomenclature

Symbols and parameters of the formulations.

$B_{e,p,j}$	electricity purchase price at interval j ($ kWh^{-1})
$B_{e,s,j}$	electricity sales price at interval j ($ kWh^{-1})
B_{Hs}	hydrogen sales price ($ kg^{-1})
B_{g1}	natural gas price as FCPP fuel ($ kWh^{-1})
B_{g2}	natural gas price for residential loads ($ kWh^{-1})
B_p	hydrogen storing cost ($ kWh^{-1})
$D_{e,j}$	electricity demand at interval j (kW)
$D_{t,j}$	thermal demand at interval j (kW)
MSI	minimum stop-time (number of intervals)
MRI	minimum run-time (number of intervals)
$n_{start-stop}$	number of start–stop events
N^{max}	maximum number of start–stop events
O&M	daily operation and maintenance cost ($)
P_a	power for auxiliary devices (kW)
P_r	power ramp rate – low limit
P_s	power ramp rate – high limit
PH,end	available stored hydrogen at the end of the day(kWh)
P_{Hj}	equivalent electric power for hydrogen production (kW)
$PH_{st}j$	stored hydrogen at interval j (kW)
PH usage,j	secondary hydrogen stream at interval j (kW)
P_j	electrical power produced at interval j (kW) minus the power for auxiliary devices.
P_{max}	maximum limit of generating power (kW)
P_{min}	minimum limit of generating power (kW)
Pt,j	thermal load produced at interval j (kW)
P_{th},reform,j	reformer recovered thermal power at interval j (kW)
P_{th},pem,j	PEM recovered thermal power at interval j (kW)
P_{total},pem,j	Overall PEM (four-stack) recovered thermal power at interval j (kW)
PT_j	total power produced at interval j, where $PT_j = P_j + P_a + P_{Hj}$
PLR	part load ratio
λ_j	thermal energy to electrical energy ratio
T	length of time interval (h)
t_{off}	time that the FCPP is off (h)
T_{off}	FCPP off-time (number of intervals)
T_{on}	FCPP on-time (number of intervals)
S	FCPP on–off status, $S = 1$ for running, $S = 0$ for stopping

Greek symbols

α,β	hot and cold start up cost, respectively
η_j	fuel cell electrical efficiency at interval j
η_{st}	hydrogen storage efficiency
τ	fuel cell cooling time constant (h)

power systems. In this research, Particle Swarm Optimization (PSO) algorithm determines the optimal strategies of FCPP which was previously tested in Ref. [11]. In this study, the FCPP provides electricity demand, with peak of 250 kW, and heat demand of a residential building which consists of fifty apartments. Four 68 kW paralleled Proton Exchange Membrane (PEM) Fuel cells, and a reformer with capacity of 100 Nm^3/hr from respectively Ballard and Mahler are used for Modeling FCPP. Impacts of reforming energy subsidies on the FCPP income are studied in Iran. Correcting factors for revising gas and electricity tariffs are proposed. Selling hydrogen from natural gas by a reformer is found as a beneficial investment in Iran.

2. FCPP configuration and energy flow strategy

Fig. 1 shows the energy flow of the FCPP model revised in Ref. [8,9] which is also applied in this study. Four Ballard fuel cells [12] with rated power of 68 kW and reformer with capacity of 100 Nm^3/hr from Mahler [13] are considered. The tank should store around 0.4 kg hydrogen per day. The flow of energy can be categorized into three different cycles: electricity, hydrogen, and heat, which are color-coded.

The system is composed of a reformer; a PEM fuel cell (PEMFC), a hydrogen-store, pumps and an inverter. Except the inverter, all components are involved in the hydrogen cycle. The reformer reforms natural gas into hydrogen to be used either as the input of PEMFC or to be stored in the hydrogen tank for future application. The stored hydrogen can be pumped into the PEMFC when hydrogen is needed. Remaining hydrogen is extracted at the end of each day and is sold. The thermal demand of a building is met by different suppliers. The national gas network is able to directly supply the building thermal load while simultaneously the thermal recovered energy of either the PEMFC or the reformer can contribute to providing the thermal load. This contribution depends on the daily operation strategy of FCPP which is determined by the daily cost function optimization. In the electricity cycle, residential building supplies its demand through the inverter of the PEMFC as well as purchasing electricity from national grid. Simultaneously, excess produced electricity can be sold to the grid. In this study, the amount of PEMFC produced electricity, the stored hydrogen and the extracted hydrogen are determined in a way that the cost function is minimum. These are optimization variables. The amount of purchased/sold electricity, thermal recovery, and gas purchased from the gas network are calculated in a post-processing analysis.

To include the hydrogen in the FCPP cost model, an equivalent electric power for produced hydrogen at each interval is assumed P_{Hj}. This power is considered at the output of the PEM terminal which allows relating the hydrogen mass and generated power with the relationship in (1).

$$(H_2)\text{amount} = 1.05 \times 10^{-8}\frac{P_{Hj}}{v_{cell}} \quad (1)$$

Amount of hydrogen is in kgs^{-1}.

Fig. 2 shows the inputs and outputs of the system. Purchased gas from the network and purchased electricity from the grid are the inputs of the system while the electricity sold to the grid, the recovered thermal energy from the PEMFC and the reformer, the hydrogen sold and the electricity produced by the PEMFC are the outputs of the system.

2.1. PEMFC thermal power

The recovered thermal power of the PEM has been calculated in Ref. [14]. The amount of electrical energy produced by the fuel cell stack is determined using the total change in enthalpy occurring in the fuel cell stack and the efficiency (η_{stack}). The chemical power released in the fuel cell stack is converted into heat (P_{th}):

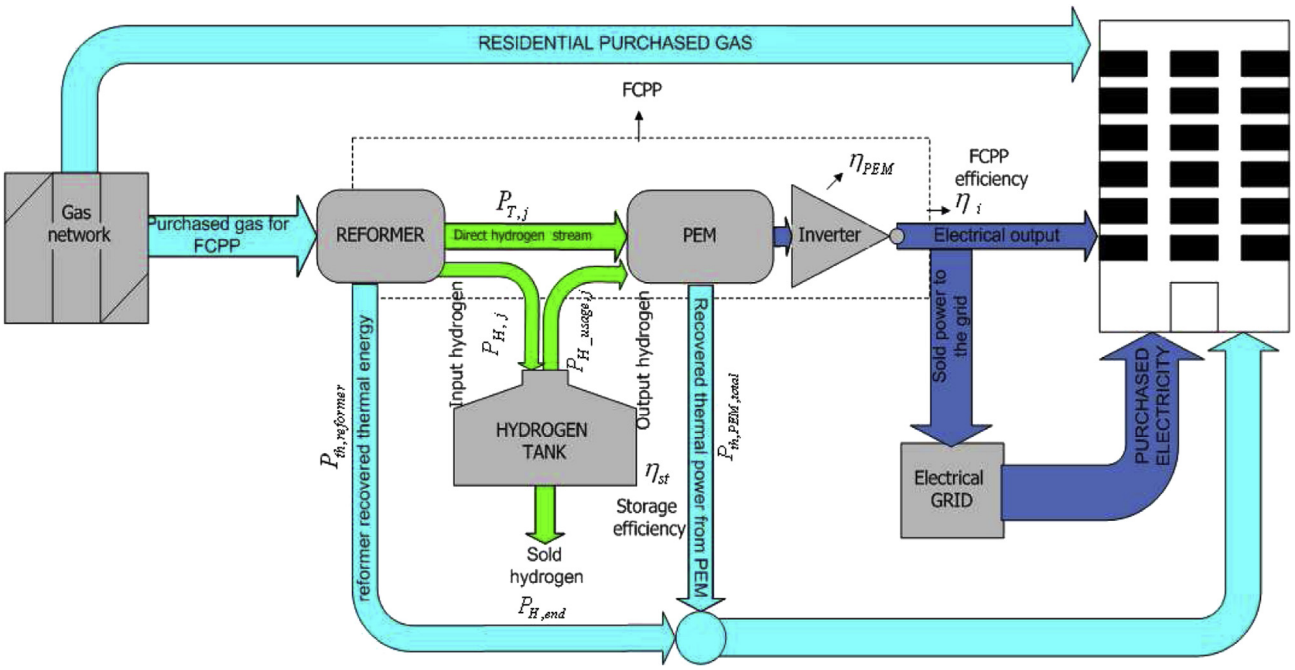

Fig. 1. System configuration; light blue, dark blue, and green colors are respectively displaying natural gas, electricity, and hydrogen stream. (For interpretation of the references to color in this figure legend, the reader is referred to the web version of this article.)

$$P_{\mathrm{j}} = \eta_{\mathrm{stack}}\,\Delta H_{\mathrm{stack}} \tag{2.a}$$

$$P_{\mathrm{th}} = \Delta H_{\mathrm{stack}} - P_{\mathrm{j}} \tag{2.b}$$

$\Delta H_{\mathrm{stack}}$ is the total change of the enthalpy in time unit. A parametric relationship is used to describe the efficiency of the fuel cell stack as a function of its electrical power output. The development of this relationship has been described previously by Ferguson and Ugursal [15].

Based on Equations (2.a and 2.b), P_{th} is present as:

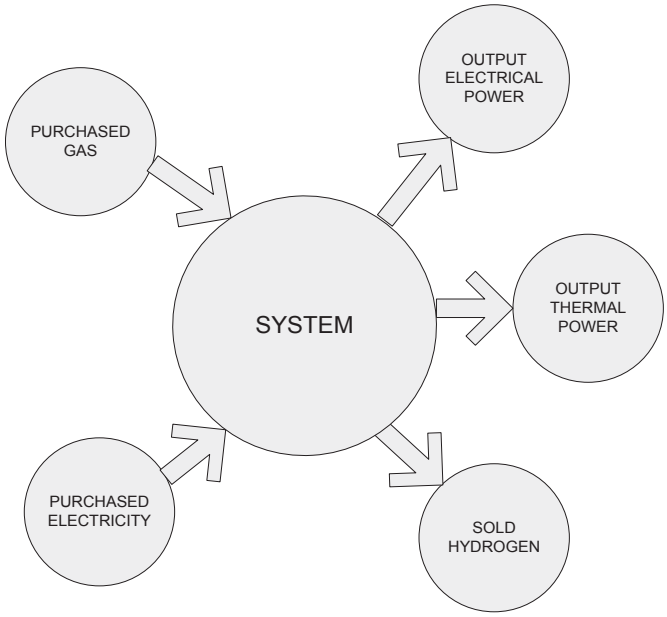

Fig. 2. Inputs and outputs of the system.

$$P_{\mathrm{th}} = \frac{P_{\mathrm{j}}(100 - \eta_{\mathrm{stack}}(P_{\mathrm{j}}))}{\eta_{\mathrm{stack}}(P_{\mathrm{j}})} \tag{3}$$

In this research, four parallel PEM with rated power of 68 kW from Ballard Company are used. The efficiency of these PEMs is calculated as:

$$\eta_{\mathrm{stack}}(P_{\mathrm{j}}) = \begin{cases} 0.875P_{\mathrm{j}} + 35.8750 & P_{\mathrm{j}} < 15 \\ -0.05P_{\mathrm{j}} + 49.7500 & 15 \le P_{\mathrm{j}} < 35 \\ -0.3666P_{\mathrm{j}} + 60.8333 & 35 \le P_{\mathrm{j}} \end{cases} \tag{4}$$

Using the efficiency expression, thermal power can be derived in (6).

$$P_{\mathrm{th,stack}} = \begin{cases} \dfrac{P_{\mathrm{j}}\left(100 - \left(\frac{7}{8}P_{\mathrm{j}} + 35.87\right)\right)}{\frac{7}{8}P_{\mathrm{j}} + 35.87} & P_{\mathrm{j}} < 15 \\ \dfrac{P_{\mathrm{j}}\left(100 - \left(-\frac{1}{20}P_{\mathrm{j}} + 49.75\right)\right)}{-\frac{1}{20}P_{\mathrm{j}} + 49.75} & 15 < P_{\mathrm{j}} < 35 \\ \dfrac{P_{\mathrm{j}}\left(100 - \left(-\frac{11}{30}P_{\mathrm{j}} + 60.83\right)\right)}{-\frac{11}{30}P_{\mathrm{j}} + 60.83} & P_{\mathrm{j}} > 35 \end{cases} \tag{5}$$

In Ref. [16] the efficiency of a suitable heat exchanger in the worst case is considered 65%. Therefore, the recovered thermal power of each PEM and overall recovered thermal power are formulated as:

$$P_{\mathrm{th,pem,j}} = 0.65P_{\mathrm{th,stack}} \tag{6}$$

$$P_{\mathrm{total,pem,j}} = 4P_{\mathrm{th,stack,j}} \tag{7}$$

2.2. Reformer thermal power

In Ref. [16] the thermal to electric output ratios of the FCPP are present. The following equations could be used for thermal recovered power of the reformer and total electrical efficiency of the FCPP:

$$\lambda_j = \begin{cases} 0.6801 & \mathrm{PLR}_j < 0.05 \\ 1.0785\mathrm{PLR}_j^4 & \mathrm{PLR}_j \geq 0.05 \\ -1.9739\mathrm{PLR}_j^3 + 1.5005\mathrm{PLR}_j^2 & \\ -0.2817\mathrm{PLR}_j + 0.6838 & \end{cases} \quad (8)$$

Recovered thermal power of the reformer is determined as:

$$P_{\mathrm{th,reform,j}} = \lambda_j (P_j + P_a + P_{\mathrm{H,j}}) \quad (9)$$

In the third model, the total recovered thermal energy of the system is the sum of the recovered thermal energy of the PEMFC and that of the reformer; (11) shows the summation.

$$P_{\mathrm{t,j}} = P_{\mathrm{total,pem,j}} + P_{\mathrm{th,reform,j}} \quad (10)$$

3. Daily cost function of the system

In Ref. [5,6], a cost function is introduced for the FCPP. In this research, the model is developed regarding the fact that the tariffs for purchasing/selling electricity are different in every hour of a day. This makes the model more realistic. This model is applied in Ref. [8,9]. Here, the output power, the retrieved thermal power, the produced hydrogen, and the power exchange are formulated as:

$$\text{Objective function} = \left(\sum \text{Cost} - \sum \text{Income}\right) \quad (11)$$

$$\begin{aligned} &\textstyle\sum \mathrm{Cost} = A + B + C + D + E + O\&M \\ &A = B_{g1} T \sum_j \left(\frac{P_j + P_a + P_{\mathrm{H,j}}}{\eta_j} \right) \\ &B = T \sum_j B_{\mathrm{e,p,j}} (D_{\mathrm{e,j}} - P_j - P_{\mathrm{H\_usage,j}}) \ \text{For} D_{\mathrm{e,j}} \geq P_j + P_{\mathrm{H\_usage,j}}, \text{else} B = 0 \\ &C = B_{g2} T \sum_j (D_{\mathrm{t,j}} - P_{\mathrm{t,j}}) \ \text{For} D_{\mathrm{t,j}} \geq P_{\mathrm{t,j}}, \text{else} C = 0 \\ &D = \sum_j (\alpha + \beta) \left(1 - e^{-\left(\frac{t_{\mathrm{off}}}{\tau}\right)} \right) \ \text{For} S_j \geq S_{j-1}, \text{else} D = 0 \\ &E = B_p T \sum_j P_{\mathrm{H,j}} \eta_{st} \end{aligned} \quad (12)$$

$$\begin{aligned} &\textstyle\sum \mathrm{Income} = F + G \\ &F = T \sum_j B_{\mathrm{e,s,j}} (P_j + P_{\mathrm{H\_usage,j}} - D_{\mathrm{e,j}}) \ \text{For} P_j + P_{\mathrm{H\_usage,j}} \geq D_{\mathrm{e,j}} \ \text{else} F = 0 \\ &G = B_{\mathrm{Hs}} P_{\mathrm{H,end}} \end{aligned} \quad (13)$$

In addition, system operation constraints are present as:

$$P^{\min} \leq P_{\mathrm{T,j}} \leq P^{\max} \quad (14)$$

$$P_{\mathrm{T,j}} - P_{\mathrm{T,j-1}} \leq P_r \quad (15)$$

$$P_{\mathrm{T,j-1}} - P_{\mathrm{T,j}} \leq P_s \quad (16)$$

$$\left(T_{j-1}^{\mathrm{on}} - \mathrm{MRI}\right)(S_{j-1} - S_j) \geq 0 \quad (17)$$

$$\left(T_{j-1}^{\mathrm{off}} - \mathrm{MSI}\right)(S_j - S_{j-1}) \geq 0 \quad (18)$$

$$n_{\mathrm{start-stop}} \leq N^{\max} \quad (19)$$

4. PSO algorithm

PSO is a population-based algorithm in which the individuals seek a known area of the search space. In this context, the population is named “swarm” and each individual is named “particle”. Each particle changes with an adjustable velocity in the search space, and keeps its previous best position in its memory. In the whole search space, the best determined position is mentioned to all of the particles [17]. For a pre-specified search space and a swarm including N particles, the position, the velocity, and the best particle position of the particle could be represented respectively by the following vectors:

$$X_i = (x_{i1}, x_{i2}, \ldots, x_{in})^T \in S \quad (20)$$

$$V_i = (v_{i1}, v_{i2}, \ldots, v_{in})^T \in S \quad (21)$$

$$P_i = (p_{i1}, p_{i2}, \ldots, p_{in})^T \quad (22)$$

Suppose that g is the index of the particle with the best position and t is the time index; therefore, the new position of the particles is calculated by the following equation:

$$V_i(t+1) = V_i(t) + cr_1(P_i(t) - X_i(t)) + cr_2(P_g(t) - X_i(t)) \quad (23)$$

$$X_i(t+1) = X_i(t) + V_i(t+1) \quad (24)$$

In which $i = 1, 2, \ldots N$ are the index of the particle, c is a positive constant known as the acceleration constant, r_1 and r_2 are random numbers in the interval [0,1] with uniform distributions [18]. In the equations of PSO, the velocity can increase without bound. This problem could be to some extent avoided by considering a maximum velocity. The following equations could be considered for updating the position and velocity of each particle:

$$V_i(t+1) = \omega V_i(t) + c_1 r_1 (P_i(t) - X_i(t)) + c_2 r_2 (P_g(t) - X_i(t)) \quad (25)$$

$$X_i(t+1) = X_i(t) + V_i(t+1) \quad (26)$$

In which ω is the so-called “inertia weight” and c_1 and c_2 are positive constants named cognitive and social parameters respectively. In (25), ω is used to reduce the effect of the previous velocity in the current velocity. Hence, ω makes a trade-off between the ability of the algorithm to find local and global optima [18,19]. In this study, c_1, c_2, and ω are 2, 2, and 0.5 respectively.

5. Software development of system modeling

In this section, development of software for related system modeling is presented. First the parameters of FCPP and PSO enter this flowchart as inputs. Next, initial values of swarms are assigned randomly. After that, based on 12 and 13, incomes and costs of the system are calculated for each particles of swarm. The system objective function is calculated in the next step. The best position that is determined by a particle up to now and its objective function value, which are obviously the best minimum value up to this point,

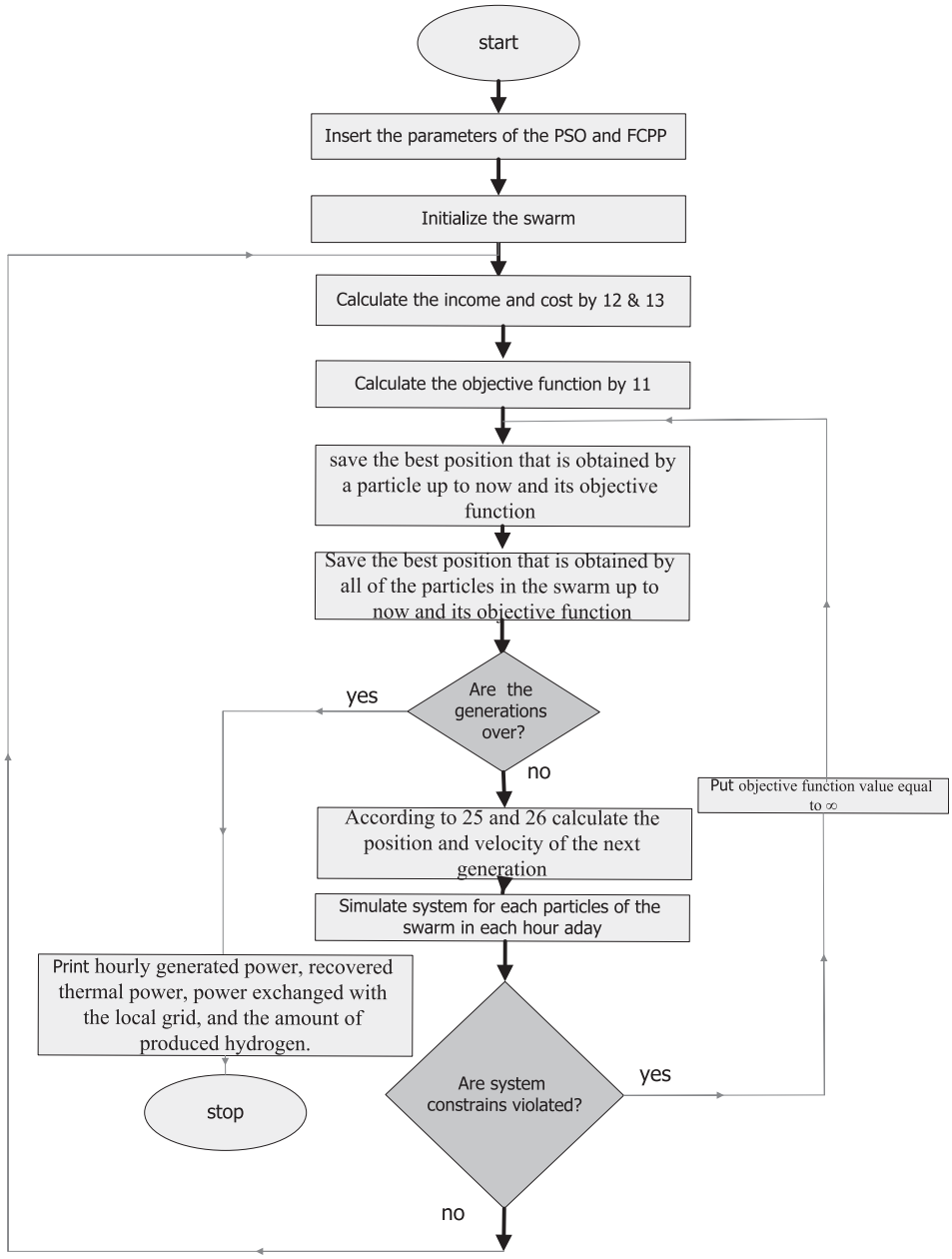

Fig. 3. Flowchart of main function (Shahverdi and Tafreshi, 2008; Shahverdi and Tafreshi, 2009).

is saved in next stage. Next, the best position that is calculated by all of the particles in the swarm up to now and its objective function will be saved. In the next step, if the number of generation is ended, function will be stopped. Else, the function continues to the end of the generation. According to (25) and (26) the position and velocity of the next generation calculated in the next step. The flowchart for the main function is shown in Fig. 3. The number of populations and generations are 700 and 1000 respectively.

6. Iran targeted subsidy plan

The Iran's subsidy reform plan was passed by Iranian parliament on January 5, 2010 [20,21]. As a main part of this plan, subsidy on energy was and still is declining, shifting energy price towards free market price in a five year period. In “Iran investment” literature, “Turquoise Partners” acknowledges that subsidy reform plan changes electricity industry into an attractive market for private investment [22]. Based on this plan, price of natural gas rises up to 75 percent of free market price (without taxes and transmission costs) by 2015; meanwhile, customers' purchased electricity tariff increases every year to eventually reach the real prime cost which is determined by competitive atmosphere of electricity market. It is obvious that the amount of energy subsidy right now is the difference between 2010 and 2015 prices.

7. Simulation and analysis results

Optimized sold/purchased electricity, hydrogen tank input/output, recovered thermal power and purchased gas for heating are variables which depict daily operational strategy of the system. Effects of Iranian reform plan on daily optimal operation of FCPP are studied in 2010–2015 period by incremental steps of one year. The

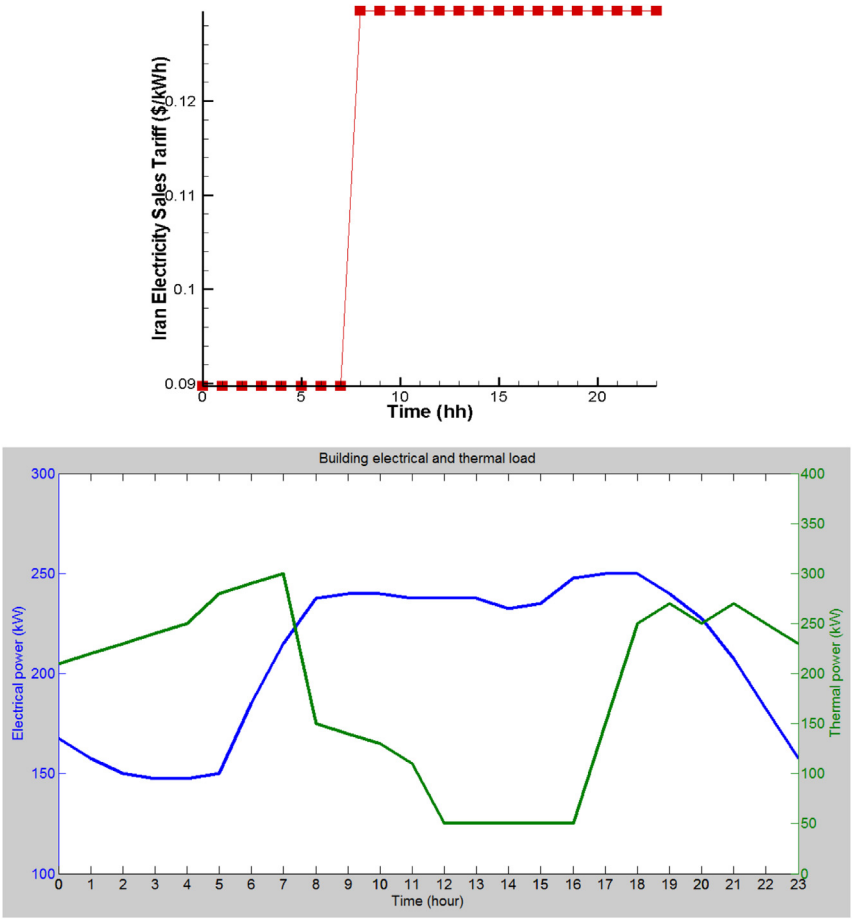

Fig. 4. 1. Iran electricity sales tariff in 2010 ($/kWh) (http://www.tavanir.org.ir). 2. Building electrical and thermal power (kW).

profile of purchased/sold electricity tariff is extracted from Tavanir organization official website, which is in charge of managing the electrical generations. Purchased electricity tariff and gas tariff were respectively 0.11 $/kWh and 0.00107 $/kWh in 2010; at the same time, sold electricity tariff is shown by Fig. 4 announced by Tavanir. In order to have a standard shape for electrical and thermal demand, IEEE-RTS daily electrical load profile by peak load of 250 kW and the typical thermal load profile extracted from Ntziachristos research are utilized in this study (see Fig. 4-2) [23]. FCPP and PSO algorithm parameters are listed in Table 1.

In this research, it is considered that energy subsidies are reduced linearly during reform years: 20 percent each year; therefore, all of the energy subsidies are removed after 5 years.

7.1. Case study one: no change in sales electricity tariff

In 2010, Iran was paying subsidies for selling energy carriers to people; thus, gas tariff and purchased electricity tariffs for consumers were at the lowest rate shown in Table 1 (0.00107 $ kWh^{-1}, 0.01107 $ kWh^{-1}). Table 2 shows that owner earns the highest earning in 2010, mainly by selling hydrogen. In the same year, Fig. 5 shows that PEMFC does not produce electricity; instead, the reformer works in full load mode to fill up the hydrogen tank and sell it at the end of the day. As a result of reformer full load operation, substantial amount of thermal energy is retrieved from reformer (Fig. 6).

Fig. 7 shows sold electrical power; as it can be seen, the FCPP sells considerably more power in peak hours comparing to the rest of time in a typical day. From 2010 to 2014, purchased power from the grid met the electrical demand of the building, and PEMFC does not produce electricity for selling to the grid excluding peak hours. However, in peak hours selling electricity tariff is higher, so selling

Table 1
FCPP and PSO algorithm default parameters.

Maximum limit of generating power, P_{max} (kW)	250
Minimum limit of generating power, P_{min} (kW)	0.00
Length of time interval, T (h)	1
Upper limit of the ramp rate, P_s (kW s^{-1})	20
Lower limit of the ramp rate, P_r (kW s^{-1})	25
2010 Price of purchased electricity, $B_{e,p,j}$ ($ kWh^{-1})	0.01107
Real price of purchased electricity, $B_{e,p,j}$ ($ kWh^{-1})	0.10982
2010 Price of natural gas for FCPP, B_{g1} ($ kWh^{-1})	0.00107
Real price of natural gas for FCPP, B_{g1} ($ kWh^{-1})	0.00665
2010 Fuel price for residential loads, B_{g1} ($ kWh^{-1})	0.00107
Real fuel price for residential loads, B_{g1} ($ kWh^{-1})	0.00665
World hydrogen selling price, B_{Hs} ($ kg^{-1})	1.80
Iran hydrogen selling price, B_{Hs} ($ kg^{-1})	125
Hot start up cost, α ($)	0.05
Cold start up cost, β ($)	0.15
The fuel cell cooling time constant, τ (h)	0.75
Minimum run-time, MRI (number of intervals)	2
Minimum stop-time, MSI (number of intervals)	2
Maximum number of start–stop time, N^{max}	5
Hydrogen storage efficiency, η_{st} (%)	95
Hydrogen storing cost, B_p ($ kWh^{-1})	0.01
Maximum number of generation	1000
Number of populations	700

Table 2
Incomes and costs of the system without changing sales tariff and during financial revolution process.

Costs and incomes during subsidy reform plan ($)	2010	2011	2012	2013	2014	2015	2010 + Iran hydrogen price
Purchased fuel cost ($)	20.02	40.99	61.76	82.72	103.68	124.45	20.02
Cost of purchased electricity ($)	55.13	148.63	251.84	350.19	432.11	0.00	55.13
Income from electricity ($)	0.00	11.99	0.00	0.00	8.75	44.06	0.00
Cost of residential purchased natural gas ($)	0.16	0.33	0.50	0.67	0.84	0.00	0.16
Hydrogen selling income ($)	651.51	624.36	651.51	651.51	624.36	73.84	45258.00
Hydrogen storing cost ($)	57.00	54.63	57.00	57.00	54.63	6.46	57.00
Total cost ($)	−519.19	−391.78	−280.41	−160.93	−41.86	13.02	−45125.68

electricity is worthwhile; and the PEMFC produces and sell the surplus to the grid.

Figs. 1, 9 and 10 verify that from 2010 to 2014, hydrogen input is at the maximum possible value; whereas, no hydrogen pumps out from the tank into the PEMFC for producing electricity. Therefore, the operational strategy is to store and sell hydrogen during these years.

From 2010 to 2014, substantial thermal energy is recovered from the reformer which is operating full load; thus, only in few hours a day does the system decide to purchase gas from the network to meet thermal demand (Fig. 11). During most hours of the day, thermal energy from the reformer supplies residential thermal demand.

In 2011, twenty percent of total energy subsidies are removed, so, obviously, the gas and purchased electricity tariff increase. However, as it is listed in Table 2, by 2014, the strategy of optimal operation remains the same.

By removing 20% of subsidies in 2011, total income of FCPP decreases (Table 2). This decrement of total income clearly will be continuing during coming years (2012–2015) since the gas and purchased electricity tariff rise yearly. The optimal operational strategy does not change through these years up to the fourth year (2014), but interesting changes happens in the fifth year (2015) (Figs. 5–11). In this year (2015), energy subsidies reform is complete and the operational strategy of the system changes. At this time, the system stops buying electricity from the grid and starts to provide the electricity required by the building on its own. This fact is obviously verified by electrical output of the FCPP plot in Fig. 5.

Referring Fig. 7, in 2015 the interesting thing is that system not only purchases no electricity from grid but also sells great amount of electrical energy to the grid (Fig. 7). This selling is predictable by accurately exploring Fig. 5, which shows PEMFC generates more than electrical demand for several hours a day. In the same year, a noticeable issue about the hydrogen path is that the system delivers majority of the produced hydrogen to PEMFC in order to have more electrical energy output. As a result of using hydrogen, only a limited amount of hydrogen is stored in the tank. Stored hydrogen is persevered in the tank for selling at the end of the day because no hydrogen is extracted from the tank (Figs. 1, 9 and 10). Fully-reforming subsidies varies the strategy of buying gas from the network for residential purposes (Table 2). What makes this change happen in the thermal cycle is that in 2015 referring to Figs. 5 and 10 the PEMFC and reformer is operating at full load, so the large amount of thermal energy is recoverable regarding Equation (10). At this year, PEMFC and reformer deliver a great amount of energy to the thermal cycle; therefore, the building does not need to purchase gas from the network for residential application (Figs. 6 and 11).

7.2. Case study two: correcting sales electricity tariff

Regarding the fact that reforming energy subsidies make a small scale power plant income smaller (section one) and referring to the commitment of the ministry of energy to small scale generators for guarantied procurement of the electricity, sold electricity tariff has to be regulated. This price should be adjusted in a way that the income of a small power plant can be at least the same income as it was in 2010. Factors for electricity sold tariffs is offered in Table 4,

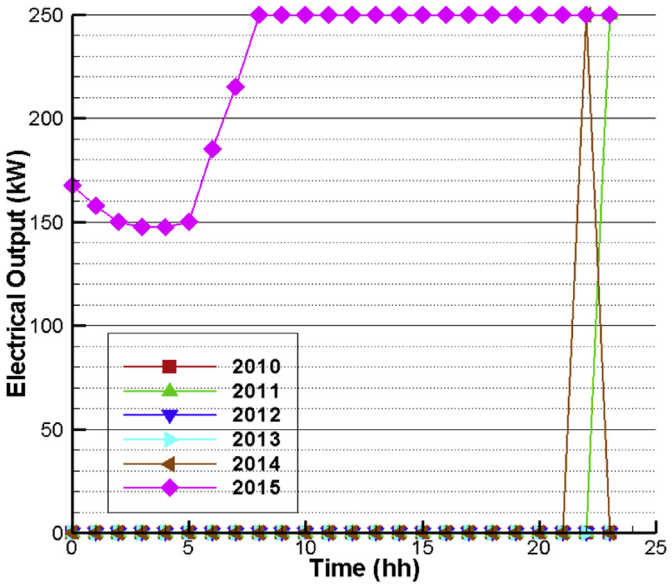

Fig. 5. Electrical output of the FCPP.

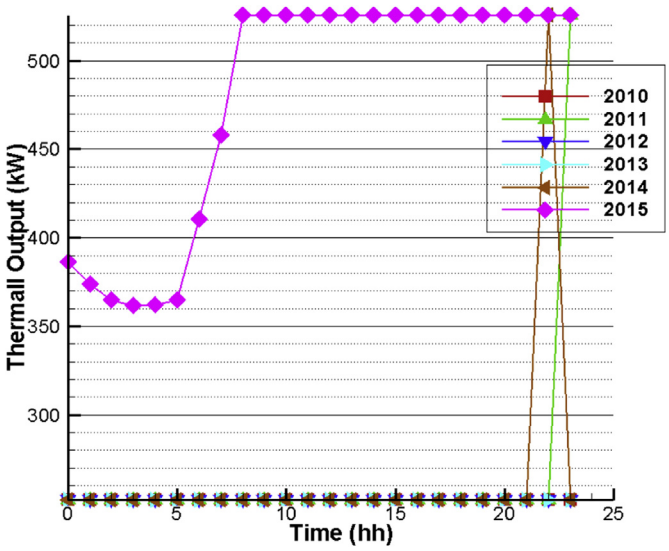

Fig. 6. Thermal output of the FCPP.

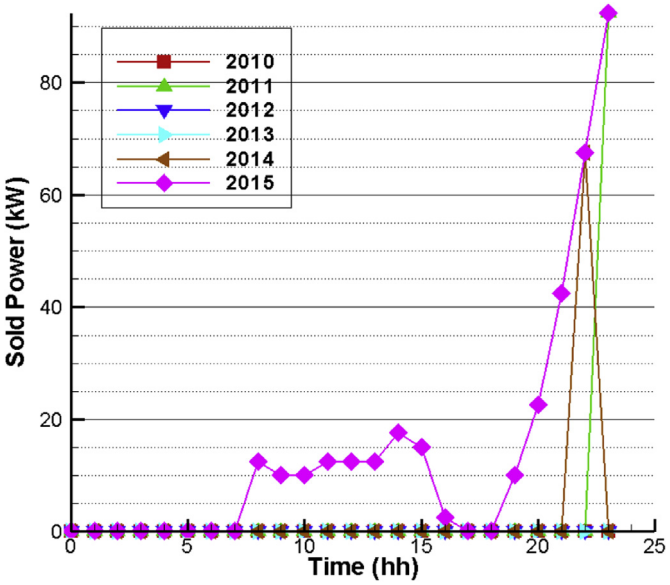

Fig. 7. Sold power to the grid.

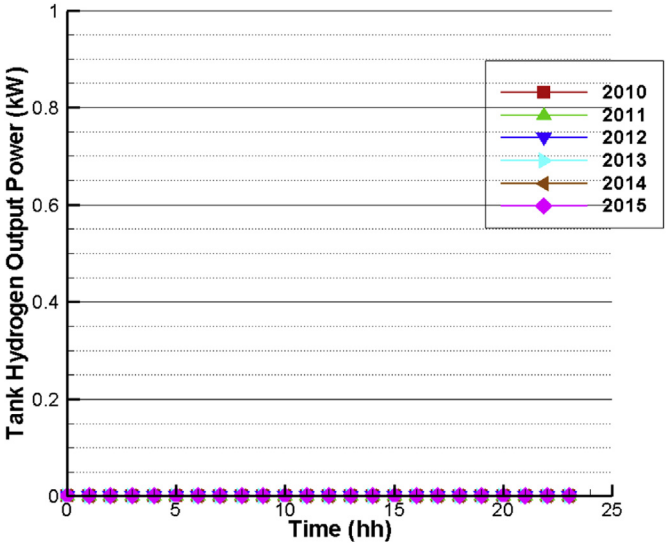

Fig. 9. Output equivalent power of hydrogen.

considering constant income from 2010 to 2015. Although these factors are calculated for FCPP, the similar trend is predictable and extendable for other small power plants. Table 3 shows how these factors make incomes stay around 2010 income (i.e., $519); other costs and incomes are also listed.

The first interesting point is that the optimization process has varied the overall operational strategy of the system after considering new sold electricity tariffs. Comparing Tables 2 and 3, respectively related to before and after setting sales factors, reveals the difference between overall strategies. After applying factors, the system earns the majority of its income by selling electricity to the grid (mainly in 2011–2015); in contrast, over the same period of time without setting factors, the system income depends mainly on selling hydrogen. By looking at Table 3, it can be observed that there are slight differences between operational strategies of each year in the period of 2010–2015, even though the overall strategy of the system, which is selling electricity, is still the same. One of the important differences is observed in Fig. 12 where PEMFC starts producing electricity at 2011, when the sales factor is 5.5. In the thermal cycle before 2011 the reformer is the only source of thermal generation, but after this year, PEMFC joins the reformer to raise the generated thermal energy to an amount even higher than the residential thermal demand (Fig. 13). This surplus thermal energy is wasted after 2011; selling this energy to neighboring buildings might be an option to increase the total income of the system.

The system does not sell electricity in Fig. 7, when no sales factor is applied, except a small amount in 2015. However, as expected, Fig. 14 shows significant electricity sold to the grid when all the subsidies are removed. This electricity is sold mostly in peak hours until early in the morning. The more sales factor and as a result sales tariff the more power on average is sold. In other words, reforming subsidies allows small scale power plants to sell more electricity.

A noticeable point here is that purchasing gas shows a decrementing yearly trend while reforming subsidies (Fig. 15).

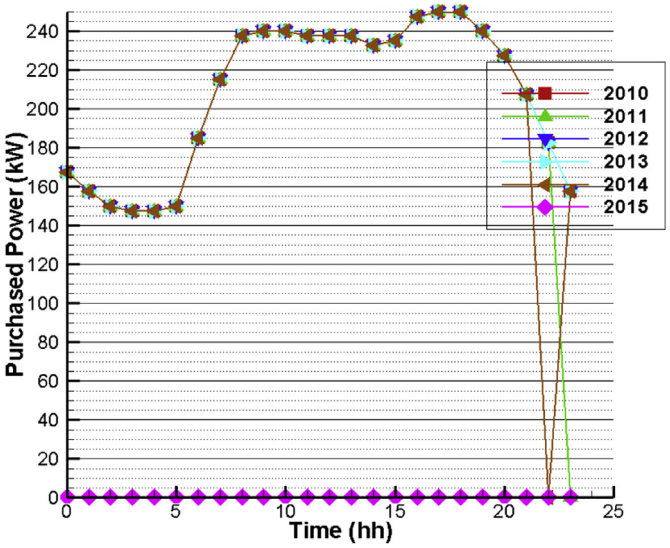

Fig. 8. Purchased power from the grid.

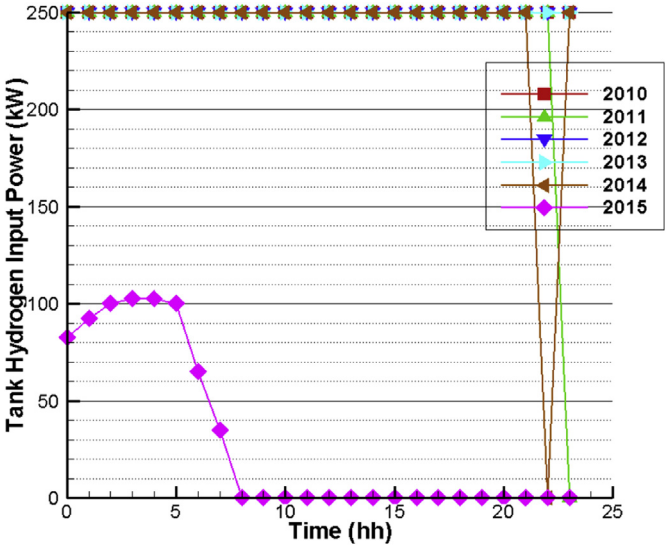

Fig. 10. Input equivalent power of hydrogen.

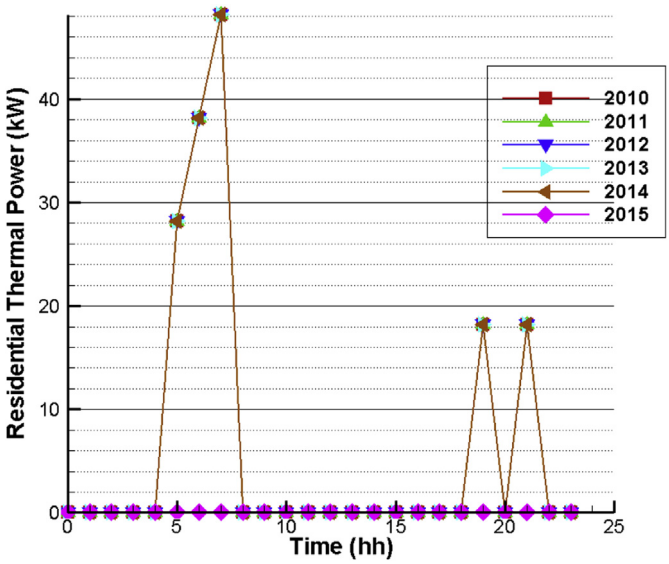

Fig. 11. Purchased gas for residential thermal load.

In the hydrogen cycle, the overall output of the hydrogen tank changes in proportion to changes in PEMFC electrical power output. In 2010, no hydrogen from the tank contributes to producing electricity, but the average of the contribution increases after 2011 (Fig. 16). Comparing Figs. 16 and 9 shows the impact of sales factor on the contribution of hydrogen in producing PEMFC electrical output.

In 2010, the electrical demand of the building is met by purchasing from the grid so the PEMFC does not play a role in producing electricity (see identical electrical power in Figs. 17 and 5) while after 2010 purchasing from grid decreases and building consumes the electricity generated internally by the FCPP.

Table 3
Incomes and costs of the system with changing sales tariff according to Table 4 and during financial revolution process.

Year	2010	2011	2012	2013	2014	2015
Purchased fuel cost ($)	20.02	39.03	59.96	81.61	102.23	118.56
Cost of purchased electricity ($)	55.13	56.53	90.68	77.68	55.55	57.62
Income from sold electricity ($)	0.00	453.62	502.33	589.24	623.25	674.05
Cost of residential purchased natural gas ($)	0.16	0.09	0.06	0.03	0.00	0.00
Hydrogen selling income ($)	651.51	193.31	196.94	119.18	72.72	45.42
Hydrogen storing cost ($)	57.00	30.58	29.39	33.59	21.55	26.25
Total ($)	−519.19	−520.71	−519.18	−515.51	−516.64	−517.04

Table 4
Calculated factors which should be multiplied by Fig. 2 to keep FCCP income constant.

Year	2010	2011	2012	2013	2014	2015
Calculated factor which should be multiplied by sales electricity price	1.00	5.50	6.00	6.80	7.24	8.00

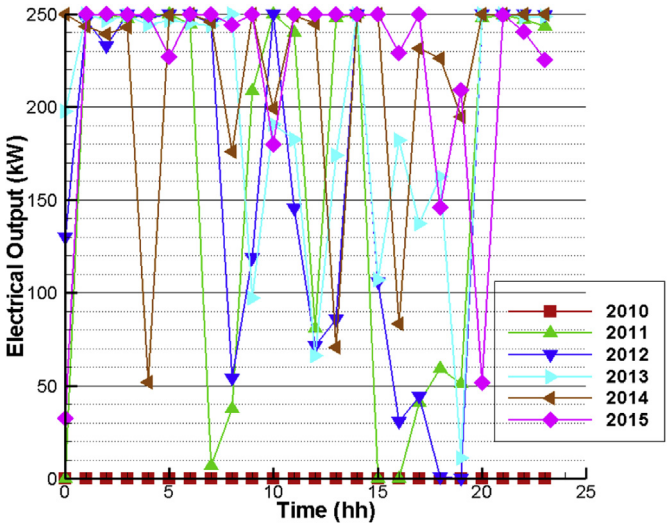

Fig. 12. Electrical output of the FCPP.

During 2011 to 2015, the optimum operational strategy of the system is similar to the first year (2011) which is shown in (Figs. 12–18 & Table 3).

An interesting point though can be found by comparing the 2010 to 2013 results (Table 3). As it can be seen, the cost of purchased electricity is growing from 2010 to 2012; but, after 2013 this cost goes down. Furthermore, the sold electricity power is decreasing at 2014, compared to 2013. These evidences show that the system prefers to supply its local load more at this time than selling to the grid. Supplying the local load does not mean that FCPP earns less money from selling electricity; the increment in sold electricity tariff compensates the deficiency in the amount sold to the grid to keep the total income constant (Table 3).

7.3. Case study three: considering Iranian hydrogen sales rate

In Section one and two, international hydrogen price was considered for analysis. For Iranian hydrogen pricing, the impacts of unit size on hydrogen price are discussed in Refs. [24]; but the real price of hydrogen in Iran is not officially known. For example in the

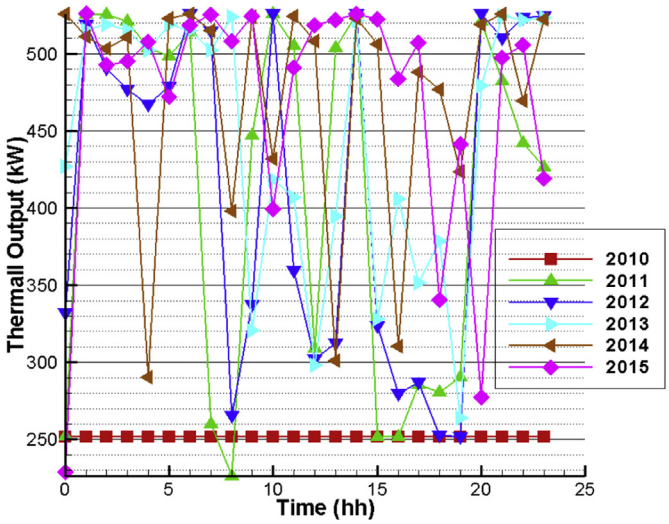

Fig. 13. Thermal output of the FCPP.

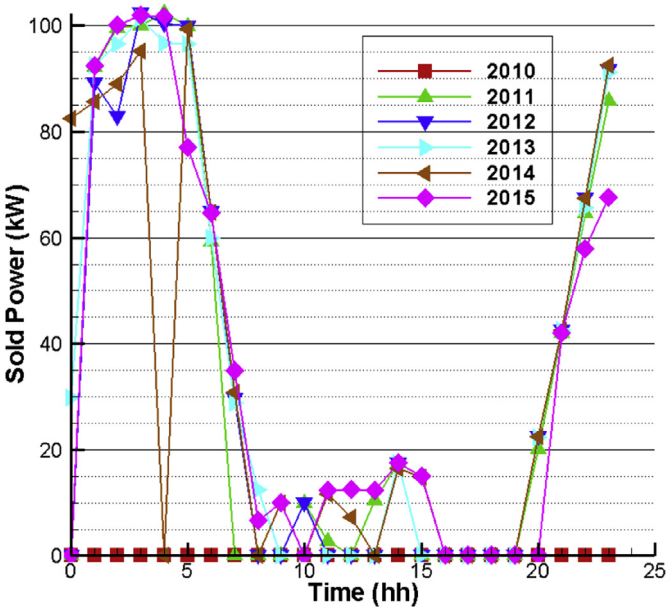

Fig. 14. Sold power to the grid.

unofficial market, it is sold at 125 $/kg. The authors briefly study here simulation results concerning Iranian hydrogen pricing. 2010 rates are considered to deliver comparable results within the fully subsidized situation. FCPP produces no electricity and the entire input energy is utilized to generate hydrogen. Optimum operational strategy is the same as that explained in section one (Figs. 5–11). The total income of the system drastically rises in this situation and a high profit might be earned by FCPP (Table 2). Fig. 19 shows the amount of input hydrogen which is stored in the limited size tank, which is considered for simulation. It should be noticed that the income in Table 2 for Iranian hydrogen price is calculated for the size hydrogen tank used in the system.

8. Conclusions and future work

The energy management of a small scale power plant was examined considering the on-going reform of energy subsidies, which is the most controversial issue in the Iranian electrical

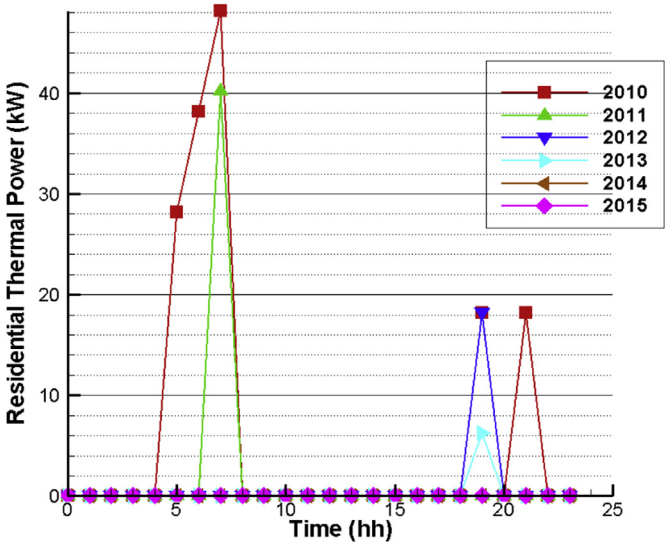

Fig. 15. Purchased gas for residential thermal load.

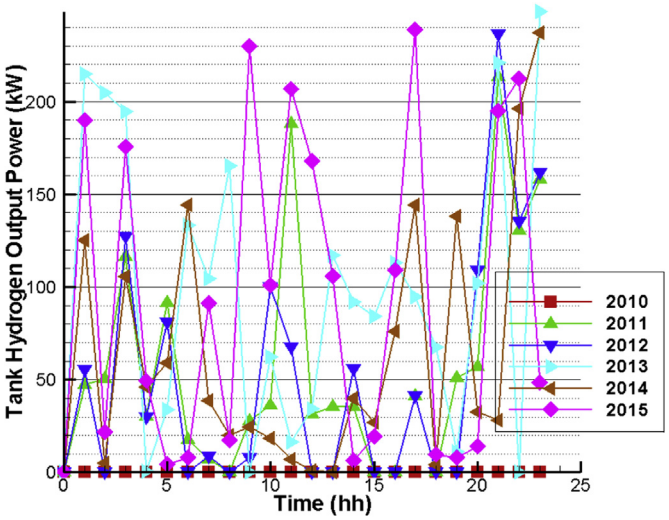

Fig. 16. Output equivalent power of hydrogen.

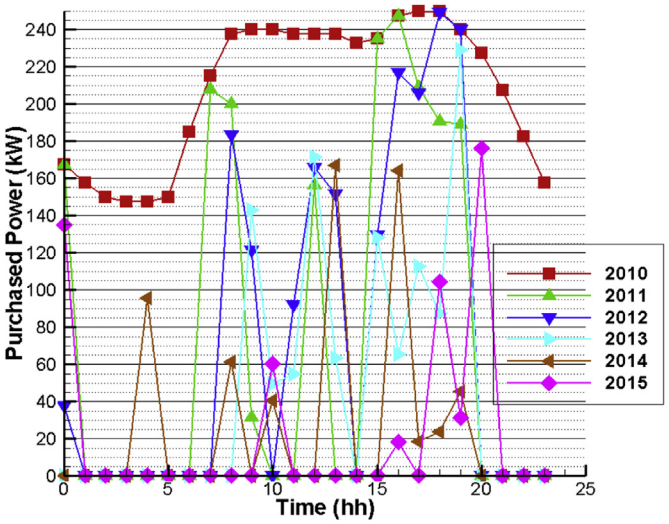

Fig. 17. Purchased power from the grid.

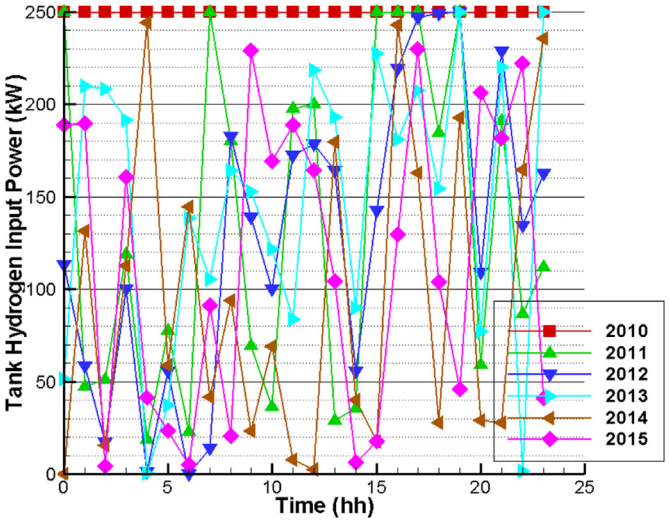

Fig. 18. Input equivalent power of hydrogen.

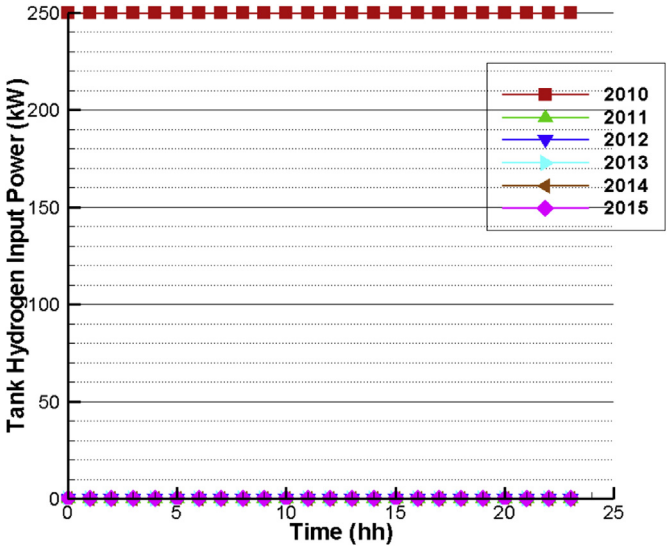

Fig. 19. Input equivalent power of hydrogen.

industry. First, in accord with the Ministry of Energy's commitment to small scale power plants, a study proposed that Tavanir organization should regulate sold electricity tariff to prevent small scale power plants from shutting down after completion of the reform of the energy subsidies. Proposed tariffs in Table 4 might be extended to small scale power plant businesses in general. Second, the hydrogen price in Iran is too high; this creates a good opportunity for installing a reformer and producing hydrogen from natural gas. A hydrogen market can be established to bring benefits to reformer owner if the considerable demand hydrogen remains in Iran. Third, the potential of producing thermal power is significantly large, in fact it is more than the thermal demand of the corresponding building during many hours of the day. One suggestion is to utilize this waste heat to run an absorption chiller, which is a cooling system that consumes excess heat.

References

[1] http://www.tavanir.org.ir: letter no. 52504/350, October 22, 2008. [Online].
[2] Maher AR, Al-Baghdadi Sadiq, Haroun AK, Al-Janabi Shahad. Parametric and optimization study of a PEM fuel cell performance using three-dimensional computational fluid dynamics model. Renew Energy 2007;32(7):1077–101.
[3] Pandiyan S, Elayaperumal A, Rajalakshmi N, Dhathathreyan KS, Venkateshwaran N. Design and analysis of a proton exchange membrane fuel cells (PEMFC). Renew Energy 2013;49:161–5.
[4] Hou Yongping, Shen Caoyuan, Yang Zhihua, He Yuntang. A dynamic voltage model of a fuel cell stack considering the effects of hydrogen purge operation. Renew Energy 2012;44:246–51.
[5] El-Sharkh MY, Tanrioven M, Rahman A, Alam MS. Cost related sensitivity analysis for optimal operation of a grid-parallel PEM fuel cell power plant. J Power Sources 2006;161(2):1198–207.
[6] El-Sharkh MY, El-Keib AA. Maintenance scheduling of generation and transmission systems using fuzzy evolutionary programming. Power Systems IEEE Trans 2003;18(2):862–6.
[7] El-Sharkh MRAAM. Evolutionary programming-based methodology foreconomical output power from PEM fuel cell for micro-grid application. J Power Sources 2005;139(1–2):165–9.
[8] Shahverdi M, Tafreshi SMM. Operation optimization of fuel cell power plant with new method in thermal recovery using particle swarm algorithm. In: IEEE DRPT, Nanjuing; 2008.
[9] Shahverdi M, Tafreshi SMM. Operation of fuel cell power plant with thermal recovery of PEM using free-model optimization. Eur J Scientific Res 2009;36(4):521–33.
[10] Azmy Ahmed M, Erlich István. Online optimal management of PEM fuel cells using neural networks. IEEE Trans Power Delivery 2005;20(2):1051–8.
[11] Niknam Taher, Meymand Hamed Zeinoddini, Nayeripour Majid. A practical algorithm for optimal operation management of distribution network including fuel cell power plants. Renew Energy 2010;35(8):1696–714.
[12] http://www.ballard.com/ [Online].
[13] http://www.mahler-ags.com/ [Online].
[14] Ferguson A, Beausoleil-Morrison I, Ugursal VI. A comparative assessment of fuel cell cogeneration heat recovery models. In: Eighth international IBPSA conference, Eindhoven, Netherlands; 2003.
[15] Ferguson A, Ugursal VI. Fuel cell modeling for building cogeneration applications. J Power Sources 2004;137(1):30–42.
[16] Gunes M. Investigation of a fuel cell based total energy system for residential applications. Master of Science Thesis. Department of Mechanical Engineering, Virginia Polytechnic Institute and State University.; 2001.
[17] Eberhart RC, Kennedy J. A new optimizer using particle swarm theory. In: Proc. 6th symp. micromachine and human science, Nagoya, Japan; 1995. pp. 39–43.
[18] Hu X, Eberhart R. Solving constrained nonlinear optimization problems with particle swarm optimization. In: 6th world multiconference on systemics, cybernetics and informatics (SCI); 2002.
[19] Parsopoulos KE, Vrahatis MN. On the computation of all global minimizers through particle swarm optimization. IEEE Trans evolutionary comput 2004;8(3):211–24.
[20] http://www.dolat.ir [Online].
[21] Presstv.com [Online].
[22] S. Shahriari, Turquoise partners: Iran investment monthly (march 2011). Retrieved april 30, 2011.
[23] Ntziachristos L, Kouridis C, Samaras Z, Pattas K. A wind-power fuel-cell hybrid system study on the non-interconnected Aegean island grid. Renew Energy 2005;30:1471–87.
[24] SD. Mohammadi-far, R. Ghyas, and B. Zarabi, Economic analysis of hydrogen production in Iran in Farsi.